Kinetics of bifunctional isomerization over carbides (Mo, W)

Anne-Félicie Lamic, Thi Lan Huong Pham, Claude Potvin *,
Jean-Marie Manoli, Gérald Djéga-Mariadassou

Laboratoire de Réactivité de Surface, Université Pierre et Marie Curie, 4 Place Jussieu, T 54-55, Case 178, 75252 Paris Cedex 05, France

Abstract

Kinetics of isomerization of n-heptane was studied over three types of catalysts: a W_2C-type carbide and two composites of molybdenum carbide and tungsten oxide. The precursors were carburized using ethane (10 vol.% C_2H_6/H_2) following a temperature programmed reaction up to 863 K. The catalytic test conditions were as follows: total pressure of 1 or 6 bar, temperature range between 543 and 623 K, and H_2/nC_7 molar ratio equal to 14.8. The selectivity towards isomers was at least equal to 89% for the full range of conversion. The global consumption of n-heptane is a first order reaction to the reactant. By simulating the global kinetics of the reaction, the experimental curves lead us to calculate rate constants. We show that, at conversion higher than 60%, the reaction becomes a two-way process. The $2mC_6/3mC_6$ molar ratio was close to 1, corresponding to a bifunctionnal isomerization. Isomerization mechanism can be explained by three cycles: the first cycle, corresponding to the dehydrogenation of the n-alkane on metallic sites, is closed to equilibrium; the second corresponds to the isomerization of n-alkene into iso-alkene on acidic sites; finally, the third cycle corresponds to the hydrogenation of iso-alkene into iso-alkane on metallic sites. We showed that the global kinetics of the reaction only occurs on acidic sites.
© 2005 Elsevier B.V. All rights reserved.

Keywords: Carbides; Bimetallic; Isomerization; n-Heptane; Two-way process

1. Introduction

New constraints on the octane number of the unleaded gasoline, as well as health and environmental protections, lead to new targets. It is necessary to develop processes allowing to obtain reformulated gasolines, in order to decrease harmful emissions, while maintaining the properties necessary to the correct operation of engine.

Transition metal carbides are well known to have catalytic properties similar to those of group VIII metals [1]. Transition metal oxides and carbides have been found to be potential materials for hydroisomerization [2,3]. It has been shown that they can become two-way catalysts with a dioxygen treatment at high temperature. In this paper, the synthesis of carbides were performed in order to limit the carburization process

and to preserve a high content of oxygen atoms from the initial oxide, so as to control the acidic function owing to these residual oxygen species. One way consists in carburizing the oxide precursor at low temperature, using ethane as carburizing agent [4].

Isomerization of n-heptane was chosen as a model reaction to test the reactivity of the catalysts in hydroisomerization of paraffins. Molybdenum carbide [5], as well as supported noble metal, follows a metallic like isomerization process, the major route being alkane hydrogenolysis, resulting in a poor selectivity in isomerization. In the presence of zeolite or acidic materials, acidic isomerization process takes place, cracking being the major route.

Tungsten oxynitrides [6] or $Pt/WO_x–ZrO_2$ [7] present a two-way isomerization behavior, where the two functions, metallic and acidic, are present.

Only a few papers have been dedicated to the kinetics of bifunctional isomerization over carbide materials. The present paper deals with the design of bifunctional catalysts

* Corresponding author.
  E-mail address: clp@ccr.jussieu.fr (C. Potvin).

and with the global kinetics of isomerization of *n*-heptane over these materials.

2. Experimental

2.1. Materials

Molybdenum oxide (MoO_3, Aldrich, 99.99%), tungsten oxide (WO_3, Acros, 99.995%) and ammonium metatungstate (($NH_4)_6W_{12}O_{39} \cdot xH_2O$), Aldrich, 99.99%) were used as precursors.

Commercial gases employed (C_2H_6, Ar, O_2 and H_2), *n*-heptane (Aldrich, 99+%) and hydrochloric acid (Carlo Erba, 37%) were used as received.

2.2. Catalyst preparation

A W_2C-type catalyst was prepared using ammonium metatungstate as a precursor: 1.5 g of ($NH_4)_6W_{12}O_{39} \cdot xH_2O$ was introduced into a tubular quartz reactor and a 10 vol.% C_2H_6 in H_2 (total flow rate = 10 L/h) was passed through the reactor. The temperature was increased from room temperature (RT) up to 500 °C (773 K) at 240 °C/h and then from 500 °C (773 K) up to 590 °C (863 K) at 60 °C/h, the reactor was kept at 590 °C for 1.5 h. The reactor was then rapidly cooled to RT under a pure dihydrogen flow. Then, the flow was switched to pure argon and the reactor was purged during 10 min. The passivation step has been performed in 1 vol.% O_2 in argon, during 1 h.

The material was analyzed by X-ray diffraction (XRD) (Fig. 1) and by elemental analysis. The nominal composition was $WC_{0.8}O_{0.7}$.

The Mo_2C–WO_2 catalyst was prepared by crushing a mixture of MoO_3 and WO_3 (W/Mo molar ratio equal to 1) in a mortar. Ethanol was added to increase dispersion [8], and subsequently evaporated at room temperature. The carburization procedure was the same as for the W_2C-type catalyst.
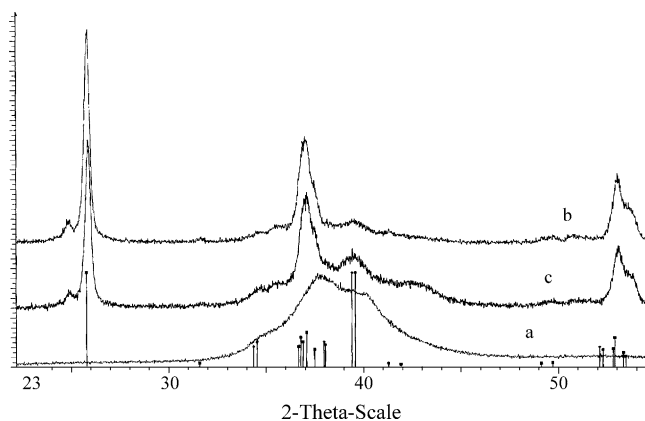

Fig. 1. XRD diffractograms for W_2C (a), Mo_2C–WO_2 (b) and $H_xMoO_yC_z$–Mo_2C–WO_2 (c). (♦) 00-035-0787 Molybdenum carbide MO_2C; (■) 00-032-1393 tungsten oxide WO_2; (●) 00-035-0076 tungsten carbide W_2C.

The temperature was raised from RT to 600 °C (873 K) at 60 °C/h and kept at this temperature for 2 h. The material was also submitted to a passivation step. It was analyzed by XRD (Fig. 1) and submitted to elemental analysis. The nominal composition was $MoWC_{0.5}O_{0.6}$.

The molybdenum bronze was synthesized using a method described elsewhere [9]. WO_3 powder was added in the same time as MoO_3 powder. The carburization step was exactly the same as for Mo_2C–WO_2 catalyst. The material was characterized by XRD (Fig. 1) and elemental analysis gave the nominal composition $HMoWO_{1.7}C_{0.5}$.

2.3. Standard reaction conditions

The isomerization of *n*-heptane was carried out in a flow reactor at either 300 °C (573 K) and 1 bar on composite materials ((Mo,W)C) or 350 °C (623 K) and 6 bar on W_2C-type catalyst. The *n*-heptane was introduced either by a high-pressure pump (Gilson) or by saturating flow of H_2 with *n*-heptane.

Temperature programmed analyses were carried out on two HP 5890 chromatograph equipped with a PONA or an Al_2O_3–KCl column, respectively.

Before reaction, (Mo,W)C materials were pretreated in situ at 500 °C in flowing H_2 (18 cm^3/min). The W_2C-type catalyst was pretreated as follows: 150 °C, 6 bar of dihydrogen, 150 cm^3/min, for 1 h.

The H_2/*n*-heptane feed ratio was set to 14.8. Contact times were calculated as the ratio between the catalyst volume (cm^3) and the total flow rate (hydrogen and *n*-heptane, cm^3/min).

3. Results

Fig. 2A shows the consumption of nC_7 and the formation of single-branched (SB) and multi-branched (MB) isomers, versus contact time, over the W_2C-type catalyst, at 350 °C (623 K) and under a total pressure of 6 bar. Similarly, the consumption of nC_7 and the production of single-branched and multi-branched isomers over $MoWC_{0.5}O_{0.6}$ and $HMoWO_{1.7}C_{0.5}$ catalysts, at 300 °C (573 K) and atmospheric pressure are reported in Fig. 2B and C, respectively. Fig. 3 shows the linear transforms of the disappearance of *n*-heptane over the three catalysts, corresponding to a global first order reaction.

On the W_2C-type catalyst, the first order reaction is observed up to a conversion of 60%. The conversion in single-branched isomers reaches a maximum and then decreases. Their concentrations go through a maximum for a contact time close to 0.27 s (Fig. 2A). At low contact time, the concentrations of multi-branched products are weak.

The reaction product distribution is given in Table 1. In all cases, the selectivity towards isomers products (defined by the percentage of nC_7 converted to *iso*-heptanes) is at least equal to 89%. The major products are monomethylhexanes
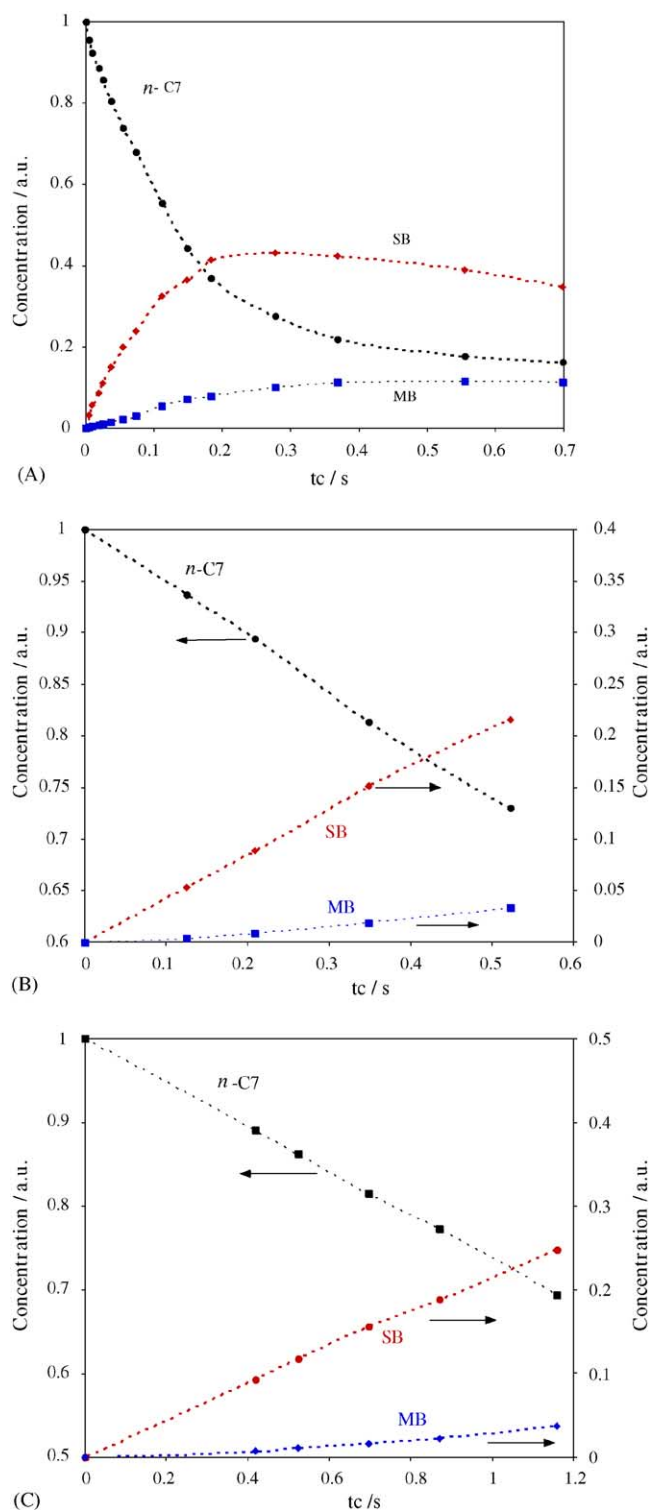
(A)

(B)

(C)

Fig. 2. Concentration of nC$_7$, SB and MB vs. contact time for W$_2$C (A), Mo$_2$C–WO$_2$ (B) and H$_x$MoO$_y$C$_z$–Mo$_2$C–WO$_2$ (C) at 350 °C (623 K) and 6 bar (A) and 300 °C (573 K) and 1 bar (B, C). Dot curves represent an interpolation of the experimental points.
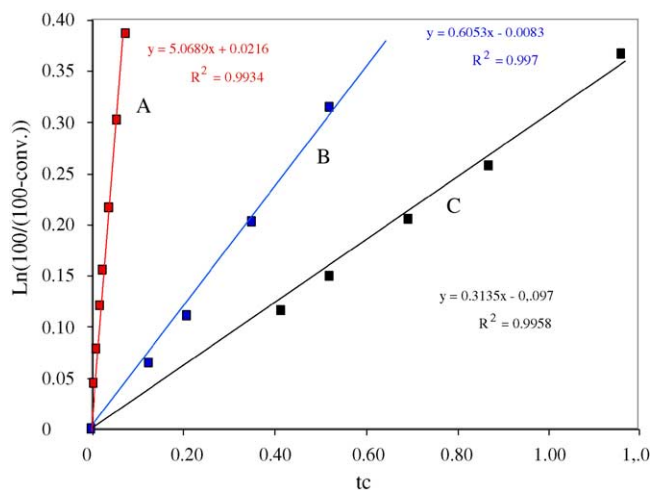

Fig. 3. Linear transformations of the consumption of nC$_7$ for W$_2$C (A), Mo$_2$C–WO$_2$ (B) and H$_x$MoO$_y$C$_z$–Mo$_2$C–WO$_2$ (C).

(2mC$_6$ and 3mC$_6$). The other reactions are hydrogenolysis, cracking and dehydrogenation.

4. Discussion

If we assumed that short linear molecules (C$_1$ + C$_2$ + C$_3$ + nC$_4$ + nC$_5$ + nC$_6$) are produced by hydrogenolysis on the metallic sites, this reaction represents less than 6% of the total n-heptane transformed, and it will be neglected in the kinetic analysis.

First of all, we observed the same kinetics whatever the catalyst (Fig. 3).

According to Table 1, the nC$_7^=$/nC$_7$ molar ratio is closed to thermodynamic equilibrium. At 6 bar and 350 °C (623 K), this ratio is equal to 2.2×10^{-3}, according to Stull et al. [10]. In our case, for the W$_2$C-type catalyst and under the same conditions, this ratio is equal to 5.8×10^{-3}. Thus, the global reaction nC$_7$ = nC$_7^=$ + H$_2$ is near thermodynamic equilibrium.

Isomerization reaction takes place on acidic sites and the global kinetic curves (first order to nC$_7$) until a conversion of 60% can be explained using the Sinfelt model, described in Fig. 4 [11].

The three cycles involve both metallic and acidic sites. There is no common adsorbed intermediate and thus these reactions are not kinetically coupled.

The first cycle represents the dehydrogenation of nC$_7$ to nC$_7^=$ over a metallic site. The corresponding sequence is

$$n\text{C}_7 + 2* \rightleftharpoons *n\text{C}_7^=* + \text{H}_2 \qquad (1)$$

$$*n\text{C}_7^=* \rightleftharpoons n\text{C}_7^= + 2* \qquad (2)$$
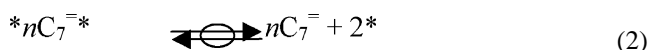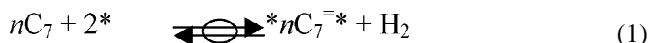
where the $*$ stands for metallic adsorption sites, both elementary steps being close to equilibrium, as previously shown. This cycle has to present a high turnover rate to deliver nC$_7^=$ to cycle 2. Consequently, the rate of disappearance of nC$_7$ must be governed by that of the second cycle which corresponds

Table 1
Products distribution in the conversion of n-heptane

Catalyst	W_2C		$Mo_2C–WO_2$		$H_xMoO_yC_z–Mo_2C–WO_2$	
T (°C)	350		300		300	
P (bar)	6		1		1	
t_c (s)	0.0184	0.055	0.21	0.52	0.41	0.87
Conversion (%)	11.3	26.1	10	26.9	10.9	22.7
Selectivity (%)	96.6	89	94	93.5	92.5	94
$2mC_6$	40.6	40.9	38.75	35.77	38.12	37.01
$3mC_6$	44	45	39.21	37.1	39.38	38.5
$2mC_6/3mC_6$	0.92	0.91	0.99	0.96	0.97	0.96
$3EtC_5$	3.4	3.4	2.9	2.8	3.0	2.9
diB	8.6	13.7	9.176	13.4	7.1	10.8
triB	0	0.1	0	0.1	0	0.06
$1C_7^=/nC_7$ experimental	5.8×10^{-3}		n.m.		5.0×10^{-4}	
$1C_7^=/nC_7$ theoretical	2.2×10^{-3}		2.3×10^{-5}		2.3×10^{-5}	
iC_4/nC_4	0.23	0.42	0.53	–	–	–

$2mC_6$: 2-methylhexane; $3mC_6$: 3-methylhexane; $3EtC_5$: 3-ethylpentane; diB: 2,2-dimethylpentane + 2,3-dimethylpentane + 2,4-dimethylpentane; triB: 2,2,3-trimethylbutane; n.m.: not measured.
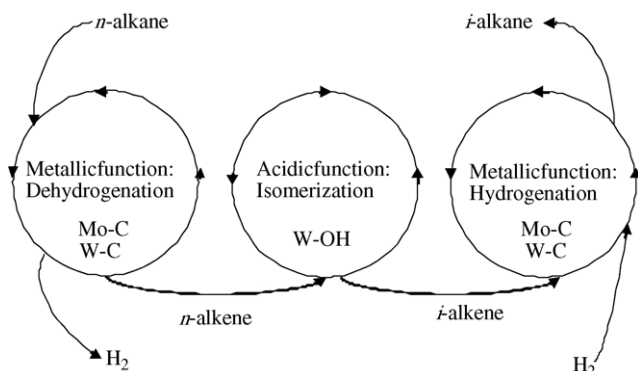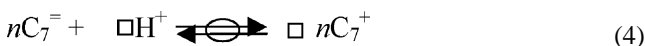

Fig. 4. Catalytic cycles representing the three functions of a two-way isomerization.

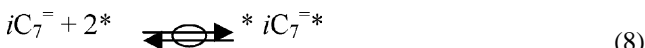to the consumption of the olefin, according to the following global reaction:

$$nC_7^= = iC_7^= \tag{3}$$

The sequence can be described as follows:

$$nC_7^= + \square H^+ \rightleftharpoons \square nC_7^+ \tag{4}$$

$$\square nC_7^+ \rightleftharpoons \square iC_7^+ \tag{5}$$

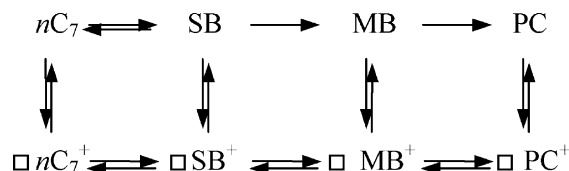$$\square iC_7^+ \rightleftharpoons iC_7^= + \square H^+ \tag{6}$$

where the $\square H^+$ stands for acidic adsorption sites.

The third cycle corresponds to the hydrogenation of $iC_7^=$ to iC_7 on metallic sites, which can be described by the following sequence:

$$H_2 + 2* \rightleftharpoons 2*H \tag{7}$$

$$iC_7^= + 2* \rightleftharpoons *iC_7^=* \tag{8}$$

$$*iC_7^=* + *H \rightarrow *iC_7H + 2* \tag{9}$$

$$*iC_7H + *H \rightarrow iC_7 + 2* \tag{10}$$

For the W_2C-type catalyst, the activation energy was found to be equal to 170 kJ/mol. This value is in agreement with that calculated over Pt/zeolite [12]. For $MoWC_{0.5}O_{0.6}$ and $HMoWO_{1.7}C_{0.5}$ catalysts, we cannot calculate the activation energy. Indeed, at temperature higher than 300 °C (573 K), the WO_2 phase undergoes a carburization (due to hydrocarbons in the reaction stream), with a subsequent change of selectivity, which prohibits any calculation of activation energy.

At conversion higher than 60%, a rake mechanism is observed, according to Guisnet et al. [13]:

$$nC_7 \rightleftharpoons SB \longrightarrow MB \longrightarrow PC$$
$$\square nC_7^+ \rightleftharpoons \square SB^+ \rightleftharpoons \square MB^+ \rightleftharpoons \square PC^+$$

For $MoWC_{0.5}O_{0.6}$ and $HMoWO_{1.7}C_{0.5}$ catalysts, contact times higher than 1.15 s cannot be obtained due to diffusion limitations.

4.1. Simulation

The experimental curves over the W_2C-type catalyst lead us to calculate rate constants by simulating the global kinetics of the reaction.

The reactional sequence considered is

$$nC_7 \underset{k_{-1}}{\overset{k_1}{\rightleftharpoons}} SB \overset{k_2}{\longrightarrow} MB + PC \tag{11}$$

The calculations with global kinetics give:

$$\frac{-d[nC_7]}{dt} = k_1[nC_7] - k_{-1}[SB] \tag{12}$$

$$\frac{d[SB]}{dt} = k_1[nC_7] - k_2[SB] - k_{-1}[SB] \tag{13a}$$

$$[SB] = \frac{1}{k_{-1}} \frac{d[nC_7]}{dt} - \frac{k_1}{k_{-1}}[nC_7]$$

$$\Rightarrow \frac{d[SB]}{dt} = \frac{1}{k_{-1}} \frac{d^2[nC_7]}{dt^2} - \frac{k_1}{k_{-1}} \frac{d[nC_7]}{dt} \qquad (13b)$$

$$\frac{d[SB]}{dt} = k_1[nC_7] - k_2 \left(\frac{1}{k_{-1}} \frac{d[nC_7]}{dt} - \frac{k_1}{k_{-1}}[nC_7] \right)$$

$$- k_{-1} \left(\frac{1}{k_{-1}} \frac{d[nC]_7}{dt} - \frac{k_1}{k_{-1}}[nC_7] \right) \qquad (13c)$$

$$\Rightarrow \frac{d[SB]}{dt} = -\frac{k_1 k_2}{k_{-1}}[nC_7] - \frac{k_2 + k_1}{k_{-1}} \frac{d[nC_7]}{dt} \qquad (14a)$$

$$(13c) = (14a) \Rightarrow \left(2k_1 - \frac{k_1 k_2}{k_{-1}} \right)[nC_7]$$

$$- \left(1 + \frac{k_2}{k_{-1}} \right) \frac{d[nC_7]}{dt}$$

$$= \frac{1}{k_{-1}} \frac{d^2[nC_7]}{dt^2} - \frac{k_1}{k_{-1}} \frac{d[nC_7]}{dt} \qquad (14b)$$

and hence

$$\frac{d^2[nC_7]}{dt^2} + (k_1 + k_{-1} + k_2) \frac{d[nC_7]}{dt} + k_1 k_2[nC_7] = 0 \qquad (15)$$

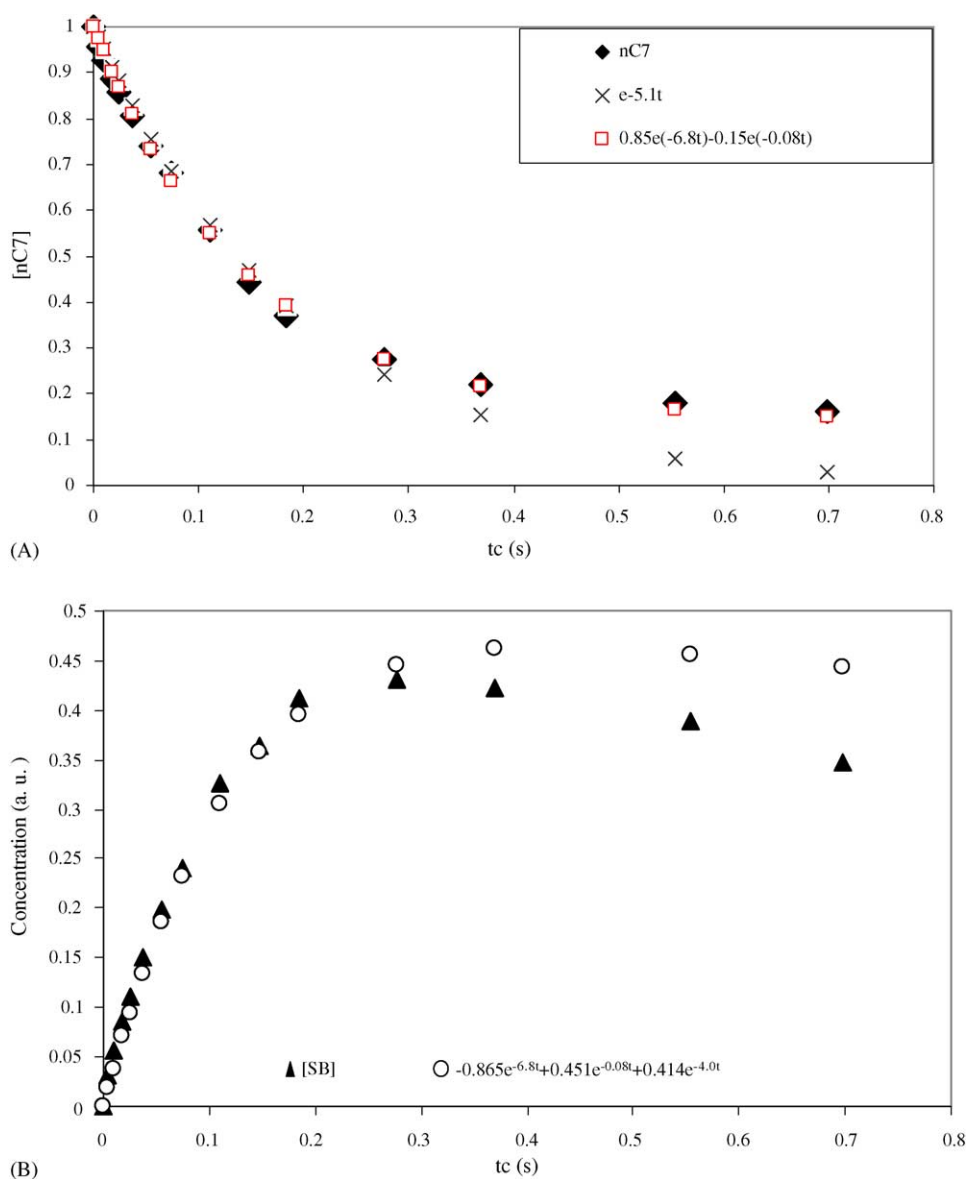Between 0 and 60% of conversion, the curve representing $[nC_7]$ versus contact time presents an exponential shape

Fig. 5. Simulated curves vs. experimental curves for nC_7 (A) and SB (B) on W_2C-type catalyst.

(Fig. 5A). The slope of the linear transformation of this curve, plotted in Fig. 5A, gives $k_1 = 5.1 \, s^{-1}$. In this range of conversion, the reaction $nC7 \to SB$ is a one-way process.

At conversion higher than 60%, the kinetics changes (Fig. 5), the rate of the reverse reaction $SB \to nC7$ (v_{-1}) becomes not negligible and the reaction becomes a two-way reaction which results in Eq. (15). The solution of such an equation is:

$$[nC_7](t) = A \, e^{x_1 t} + B \, e^{x_2 t} \qquad (16)$$

where x_1 and x_2 are the solutions of the following equation:

$$x^2 + (k_1 + k_{-1} + k_2)x + k_1 k_2 = 0 \qquad (17)$$

giving

$$x_{1,2} = -\frac{(k_1 + k_{-1} + k_2) \pm \sqrt{(k_1 + k_{-1} + k_2) - 4k_1 k_2}}{2} \qquad (18)$$

The equation of the simulated curve of the consumption of n-heptane is

$$[nC_7](t) = 0.85 \, e^{-6.8t} + 0.15 \, e^{-0.08t} \qquad (19)$$

This equation has a real kinetic signification: the first exponential represents the transformation of n-heptane into SB and the second represents the reverse reaction $SB \to nC_7$.

Moreover, at $t = 0$, we have $[nC_7](0) = 1$.

Using the simulated curves, we obtained: $x_1 = -0.08$, $x_2 = -6.8$, with $k_1 = 5.1 \, s^{-1}$.

By linear combinations of the expressions of x_1 and x_2, the values of the kinetics constants are determined as $k_1 = 5.1 \, s^{-1}$, $k_{-1} = 1.67 \, s^{-1}$, $k_2 = 0.11 \, s^{-1}$.

It is worth noting that $k_1 + k_{-1} = 6.87$, and this value corresponds to the parameter 6.8 existing in Eq. (19): $[nC_7](t) = 0.85 \, e^{-6.8t} + 0.15 \, e^{-0.08t}$. It is representative of a classical two-way reaction.

Using these values to simulate the evolution of the SB concentration (Fig. 5B), a good fitting of the experimental plot was obtained up to 70% conversion. For higher conversion, the system becomes more complex, the $SB \to nC7$ (v_{-1}) becoming too high and step 1 being a two-way process.

For the other catalysts, the conversion is not sufficiently high and only k_1 could be calculated: for Mo_2C–WO_2, $k_1 = 0.6 \, s^{-1}$; for $HMoWO_{1.7}C_{0.5}$–Mo_2C–WO_2, $k_1 = 0.47 \, s^{-1}$.

5. Conclusions

Three catalysts were used for n-heptane isomerization: W_2C, $MoWC_{0.5}O_{0.6}$ and $HMoWO_{1.7}C_{0.5}$. These carbides were synthesized using ethane as a carburizing agent for a lower temperature of carburization in order to preserve a high amount of oxygen species during the synthesis.

Kinetics of isomerization of n-heptane has been studied. The main products are single-branched isomers ($2mC_6$ and $3mC_6$). The ratio $2mC_6/3mC_6$ is close to 1, indicating that the three materials are two-way catalysts. The isomerization mechanism is a classical mechanism involving two functions – the metallic (carbide) and acidic (W–OH) ones – and three non-coupled catalytic cycles. In the first cycle, n-heptane is dehydrogenated to n-heptene on the metallic site. In the second cycle, n-heptene diffuses to an acidic site where it is isomerized, involving successive steps, and, during the third cycle, the resulting unsaturated isomers migrate to a metallic site to be hydrogenated.

It is shown that, whatever the catalyst, isomerization corresponds to a global first order reaction in respect to n-heptane, and the selectivity in isomerization products is high (at least 89%). By using the simulation of the curves of disappearance of nC_7 and appearance of the SB, the first step (transformation of nC_7) is shown to be a two-way process. It is then possible to calculate the different rate constants.

By changing the nature of the metallic phase and providing a high hydrogenating function, this study shows that the kinetics is governed by the isomerization step occurring on the acidic sites, W–OH.

References

[1] L. Volpe, M. Boudart, J. Sol. State Chem. 59 (1985) 348.
[2] F.H. Ribeiro, M. Boudart, R.A. Dalla Betta, E. Iglesia, J. Catal. 130 (1991) 498.
[3] F. Garin, V. Keller, R. Ducros, A. Muller, G. Maire, J. Catal. 166 (1997) 136.
[4] L.H. Green, in: G.F. Froment, B. Delmon, P. Grange (Eds.), Hydrotreatment and Hydrocracking of Oil Fractions, Elsevier Science, 1997, p. 485.
[5] P. Pérez-Romo, C. Potvin, J.-M. Manoli, G. Djéga-Mariadassou, Stud. Surf. Sci. Catal. (2000) 130.
[6] P. Pérez-Romo, C. Potvin, J.-M. Manoli, G. Djéga-Mariadassou, J. Catal. 205 (2002) 191.
[7] J.W. Hightower, W.N. Delgass, E. Iglesia, A.T. Bell, Stud. Surf. Sci Catal. (1996) 101.
[8] C.C. Yu, S. Ramanathan, S.T. Oyama, J. Catal. 173 (1998) 1.
[9] C. Bouchy, C. Pham-Huu, B. Heinrich, C. Chaumont, M.J. Ledoux, J. Catal. 190 (2000) 92.
[10] D.R. Stull, E.F. Westrum, G.C. Sinke, The Chemical Thermodynamics of Organic Compounds, Wiley, New York, 1978.
[11] J.H. Sinfelt, H. Hurwitz, J.C. Rohrer, J. Phys. Chem. 64 (1960) 892.
[12] P. Raybaud, A. Patrigeon, H. Toulhoat, J. Catal. 197 (1) (2001) 98–112.
[13] F. Guisnet, F. Alvarez, G. Gianetto, G. Pérot, Catal. Today (1987) 1.